

# Identifying ribosome heterogeneity using ribosome profiling (Supplementary Document)

Ferhat Alkan<sup>1,\*</sup>, Oscar G. Wilkins<sup>2,3</sup>, Santiago Hernández-Pérez<sup>1,†</sup>, Sofia Ramalho<sup>1</sup>,  
Joana Silva<sup>1</sup>, Jernej Ule<sup>2,3,4</sup>, William J. Faller<sup>1,‡</sup>

<sup>1</sup>Division of Oncogenomics, The Netherlands Cancer Institute, Amsterdam, The Netherlands

<sup>2</sup>The Francis Crick Institute, London, UK

<sup>3</sup>UCL Queen Square Motor Neuron Disease Centre, Department of Neuromuscular Diseases, UCL  
Queen Square Institute of Neurology, UCL, London, UK

<sup>4</sup>UK Dementia Research Institute Centre, King's College London, London, UK

## List of Figures

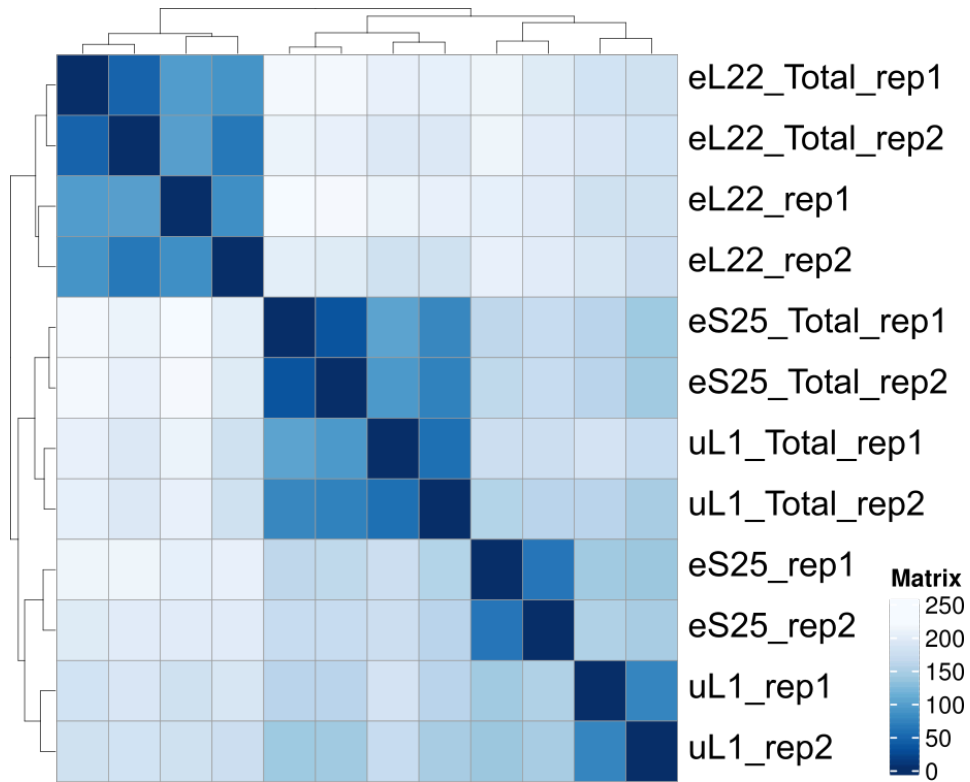
Supplementary Figure 1	2
Supplementary Figure 2	3
Supplementary Figure 3	4
Supplementary Figure 4	5
Supplementary Figure 5	6
Supplementary Figure 6	7
Supplementary Figure 7	7

---

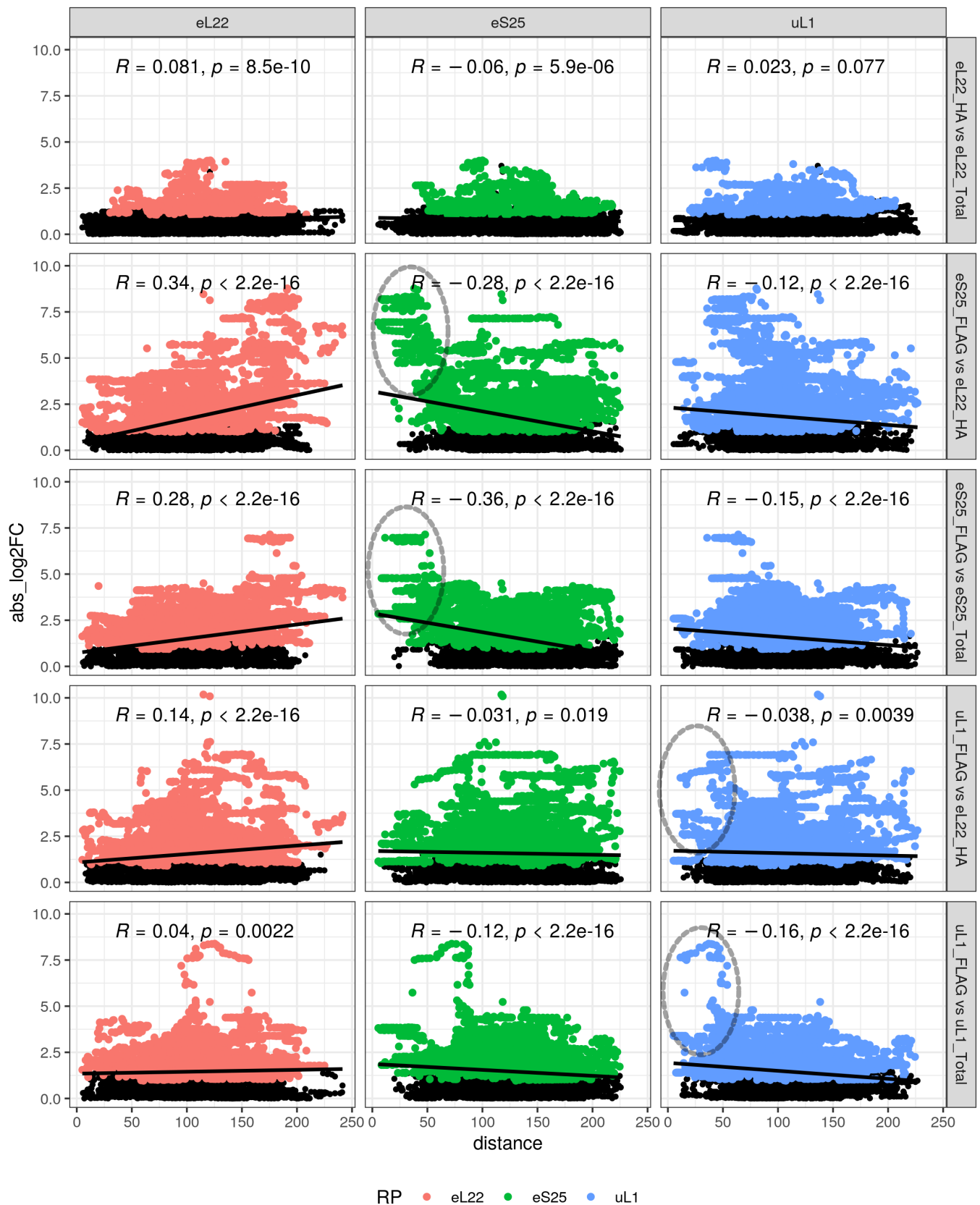
\*Software-related correspondence should be addressed to f.alkan@nki.nl

†Present address: NanoString Technologies Inc., Amsterdam, The Netherlands

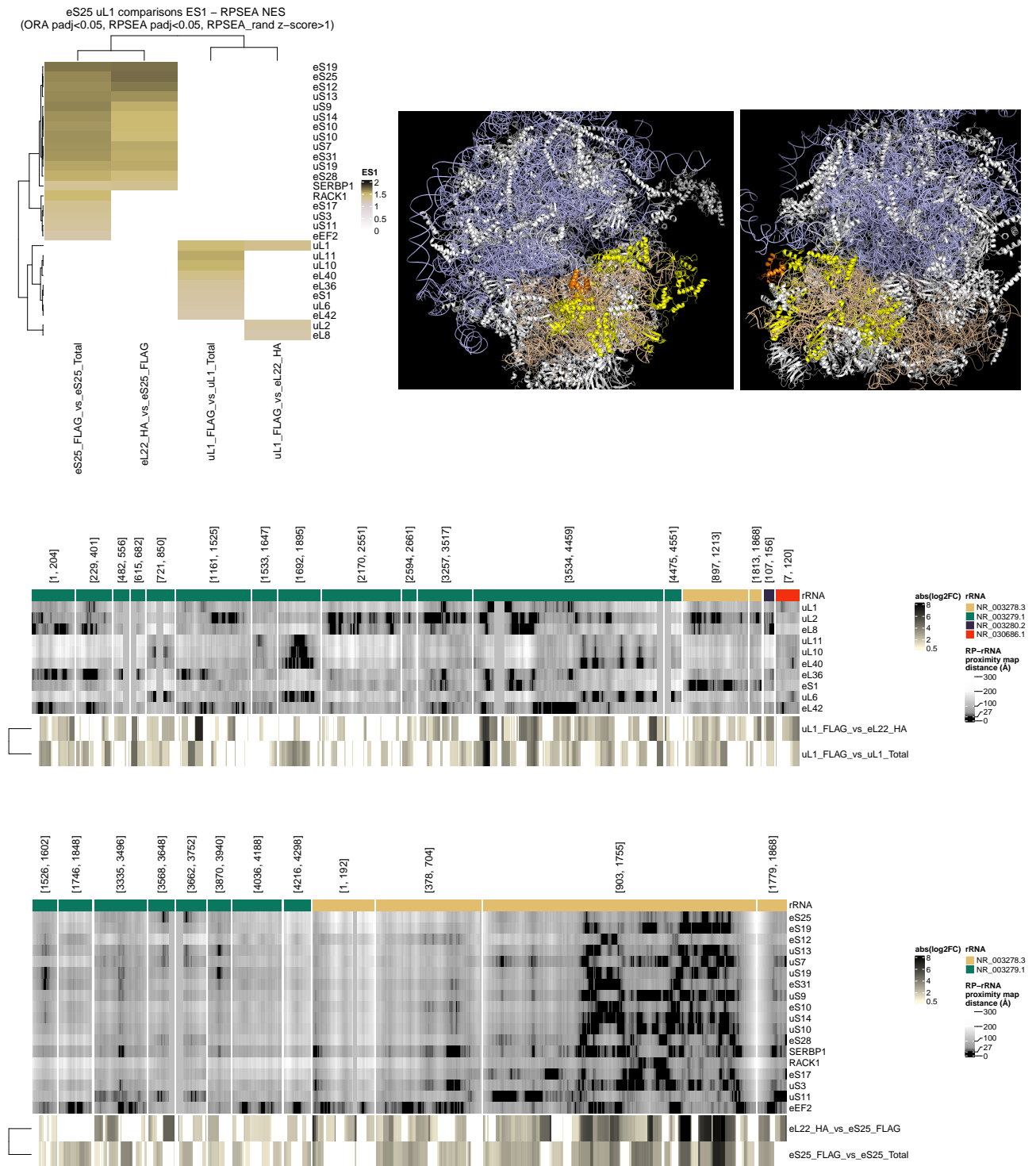
‡Corresponding Author, email: w.faller@nki.nl



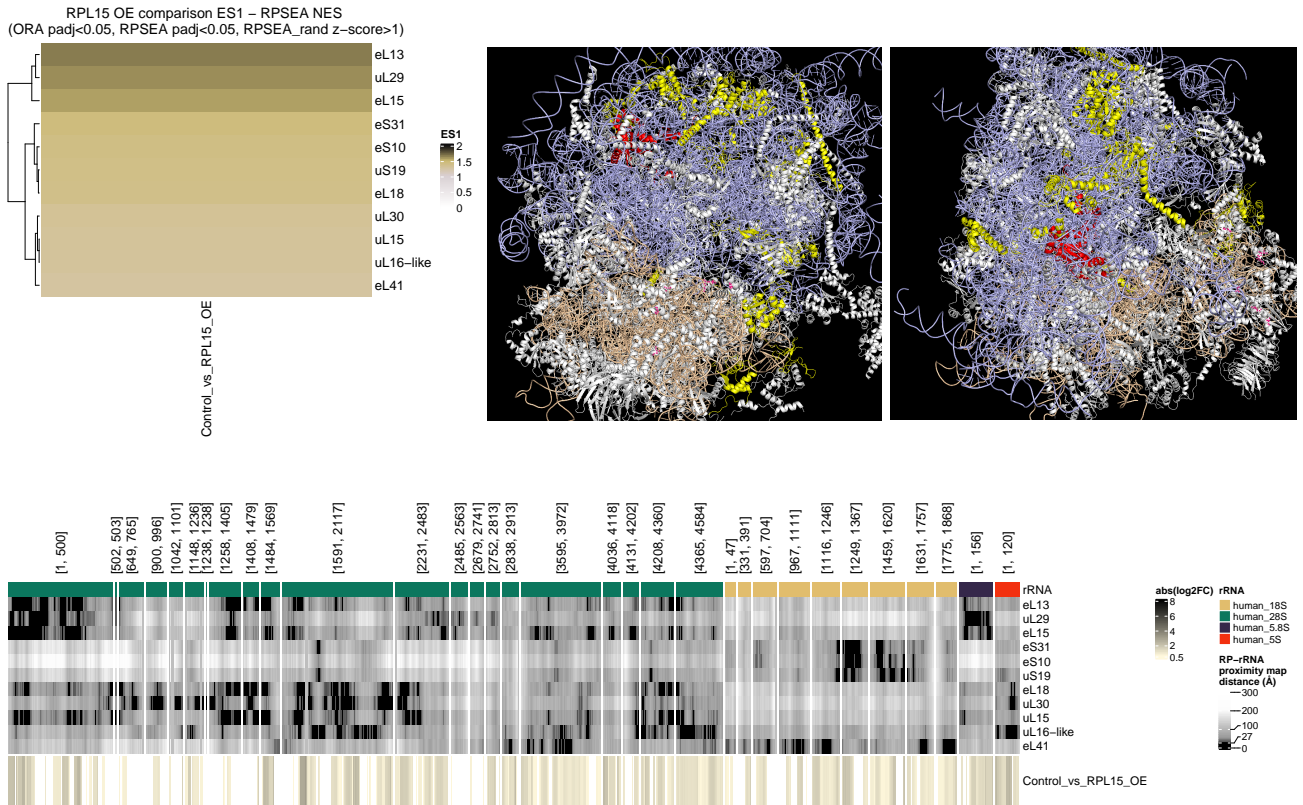
**Supplementary Figure 1:** Sample similarity distance matrix (hierarchical clustered) created with positional rRNA abundance measures for the Ribo-seq dataset with heterogeneous ribosome populations analyzed in Fig 1b-d, 2c & 3b.



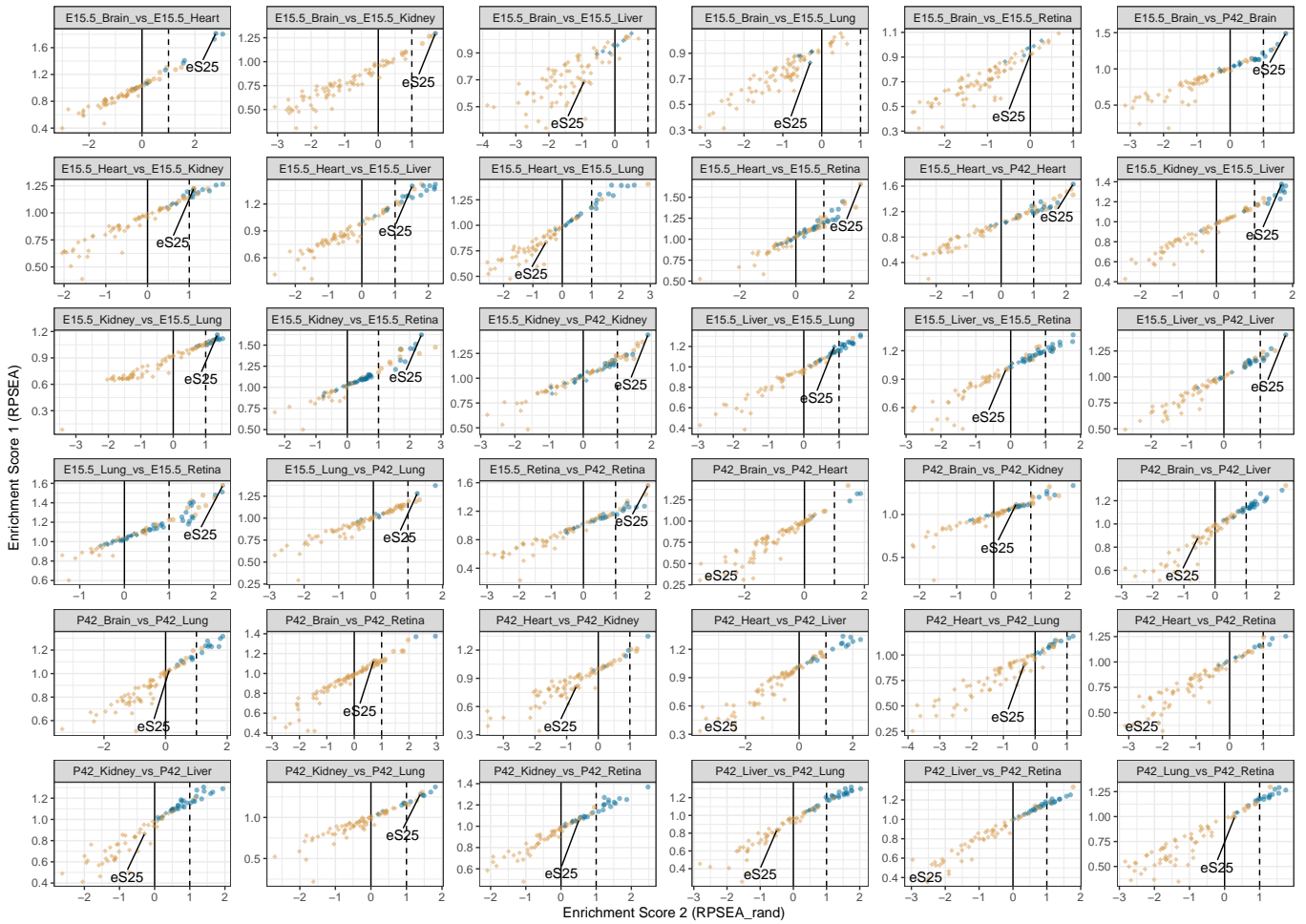
**Supplementary Figure 2:** RP-specific RP-rRNA distance vs comparison-specific rRNA abundance change scatter plots with Ribo-seq data from different ribosome populations. Each point represents a rRNA position, y-axis shows the rRNA fragment abundance change at that position and x-axis shows the distance to selected RP (eL22, eS25, eL1). Black color represent the rRNA positions that are not changing significantly and expected rRNA abundance changes in RP-proximal regions are highlighted in a dashed ellipse.



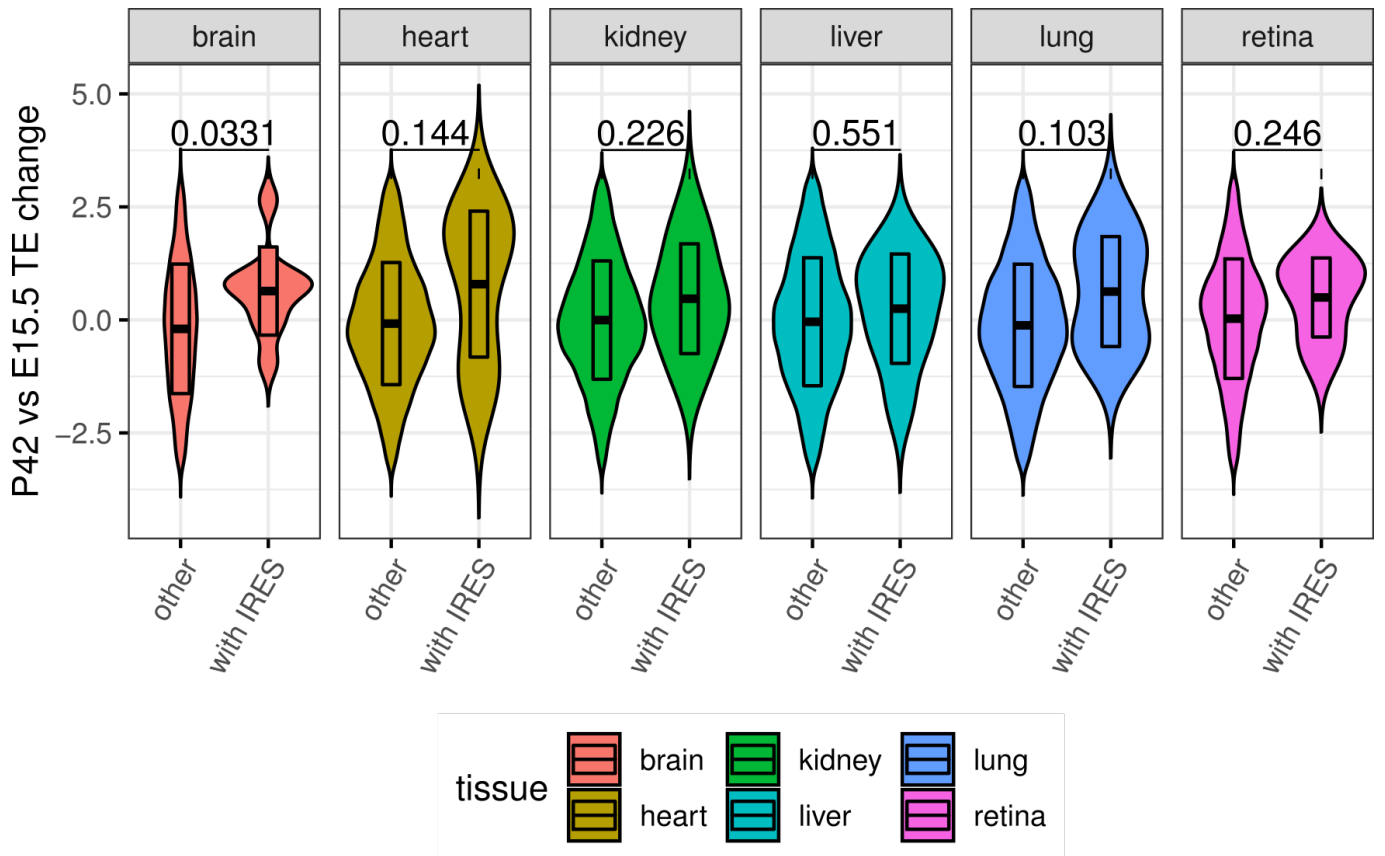
**Supplementary Figure 3: Top-left:** dripARF ribosome heterogeneity prediction results between selected populations that are given in x-axis. Heatmap color corresponds to Enrichment Score 1 of RPs given in the y-axis, where insignificant results are filtered out. **Top-right:** For eS25\_FLAG comparisons, location of predicted RP overlaps (yellow) are shown within the 3D ribosome. Orange color shows the eS25/RPS25, light blue corresponds to the 28S rRNA, and wheat color shows the 18S rRNA. **Bottom:** Two heatmaps, generated separately for eS25 and uL1 comparisons, show the location-specific rRNA abundance change and their overlap with the RP-rRNA proximity map. Layout is same as Fig. 2c in the original paper.



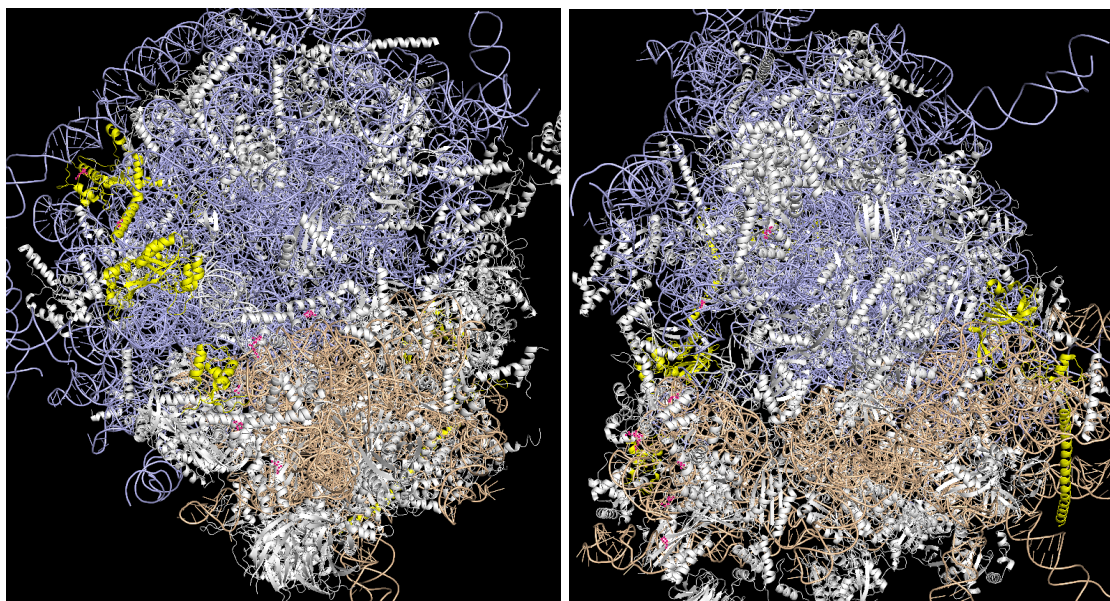
**Supplementary Figure 4: Top-left:** dripARF ribosome heterogeneity prediction results between eL15/RPL15 overexpression and WT samples. Heatmap color corresponds to Enrichment Score 1. **Top-right:** Ribosomal location of the predicted RPs are highlighted with yellow within the 3D ribosome, whereas eL15/RPL15 is shown in red, light blue corresponds to the 28S rRNA, and wheat color shows the 18S rRNA. **Bottom:** Location-specific rRNA abundance change and their overlap with the RP-rRNA proximity map. Layout is same as Fig. 2c in the original paper.



**Supplementary Figure 5:** dripARF ribosome heterogeneity prediction results for all fetal and adult tissue comparisons. One can observe that eS25/Rps25 is consistently predicted between adult and fetal stages of organs and across fetal tissue comparisons, however, not predicted in adult tissue comparisons.



**Supplementary Figure 6:** TE change (y-axis) distribution of genes in adult-vs-fetal comparisons where genes are grouped on the x-axis based on whether they contain an IRES element or not. P-values are given on top when two distributions are compared.



**Supplementary Figure 7:** We show that eS25/RPS25, eL1/RPL10A, eL13/RPL13 and eS6/RPS6 (all in yellow) are found on the periphery of the ribosome.